Emission of an atom inside a one-dimensional atomic cavity

Chaofan Zhou,[1] Yusef Maleki,[1] Zeyang Liao,[2] and M. Suhail Zubairy[1]
[1]*Institute for Quantum Science and Engineering (IQSE) and Department of Physics and Astronomy, Texas A&M University, College Station, Texas 77843-4242, USA*
[2]*School of Physics, Sun Yat-sen University, Guangzhou 510275, People's Republic of China*

(Received 7 November 2022; accepted 30 June 2023; published 18 July 2023)

We study the emission of a single-photon by a two-level emitter inside an atomic cavity consisting of two atomic mirrors coupled to a one-dimensional waveguide. With proper atomic separations, we realize a frequency comb as well as spectrum narrowing in the waveguide with the symmetric setting, and also unidirectional spectrum narrowing with asymmetric parameters. Within a suitable range, we can control the central frequency of the narrowed spectra by modulating atomic separations. Due to the collective interaction among the emitters, entanglement sudden birth and revival are observed between the mirrors.

DOI: 10.1103/PhysRevA.108.013708

I. INTRODUCTION

Photons are known to be ideal candidates for quantum information processing tasks due to their versatile capabilities and their potential as remarkable carriers of quantum information [1]. However, photons rarely interact with each other, which becomes a major problem in constructing quantum information devices from pure photon systems. The interaction between photons usually resorts to the interaction with atoms. However, the interaction between single photons and atoms is usually small in free space. To enhance their interactions, one possible solution is to confine the photons in a cavity with a high-quality factor, which is known as cavity quantum electrodynamics (cavity QED) [2–10]. The traditional optical cavity consists of two mirrors with high reflectivity, which is, however, difficult to integrate into a photonic chip [11–13].

Photonic structures with reduced dimensions, such as one-dimensional (1D) photonic waveguides, can also enhance the photon-atom interaction due to the Purcell effect [14,15]. Moreover, the photons can propagate along the waveguide, which can play the role of a quantum channel for the construction of a quantum network [16–19] and scalable quantum computation [20–26]. As a result, waveguide quantum electrodynamics (waveguide QED) has attracted considerable attention in recent years [27–45]. The atoms coupled to 1D waveguides can generate long-range dipole-dipole interactions [46–49] and can form superradiant or subradiant states depending on the atomic separation [50–54]. Due to the collective effect, an atomic array with a nearest-neighbor separation of integer times the wavelength can have a very high reflectivity for a photon pulse even with finite bandwidth [46], and two such atomic arrays can form a high-quality atomic cavity [55–57]. A single-photon frequency comb can also be generated using the atomic cavity [58–60].

In this work, we study the single-photon emission from a two-level emitter inside an atomic cavity coupled to a one-dimensional waveguide. With appropriate atomic separations, we realize a frequency comb as well as spectrum narrowing in the waveguide with the symmetric setting, and also unidirectional spectral confinement with asymmetric parameters. We show that the modulation of the atomic separations provides the tools to control the central frequency of the narrowed spectra. We also consider the entanglement between the mirrors of the cavity, and we show that entanglement sudden birth and revival can be observed between the mirrors.

The article is organized as follows. In Sec. II we formulate the model of the single-photon emission inside an atomic cavity, and we derive the corresponding solutions. In Sec. III we show the narrowing and the modulation of the output spectra. In Sec. IV we derive the concurrence of the bipartite entanglement between side emitters. In Sec. V we discuss the case with multiple-atom mirrors. Finally, we summarize the results.

II. MODEL AND THEORY

In the configuration considered in this work, an atomic array is coupled to a 1D photonic waveguide (see Fig. 1). Each emitter is considered as a two-level system with the transition frequency ω_a. The emitter inside the cavity is initially in the excited state, while all the other emitters forming the mirrors are initially in the ground state. In other words, the middle emitter emits a photon, and the side emitters form two mirrors on both sides, forming an atomic cavity in the waveguide. Considering the rotating-wave approximation, the Hamiltonian of the system is

$$H = \frac{\hbar}{2}\left(\omega_a - i\frac{\gamma}{2}\right)\sum_{j=1}^{N}\sigma_j^z + \hbar\sum_k \omega_k a_k^\dagger a_k + \hbar\sum_{j=1}^{N}\sum_k (g_k e^{ikr_j} a_k \sigma_j^+ + g_k^* e^{-ikr_j} a_k^\dagger \sigma_j^-), \quad (1)$$

where the first term is the atomic energy, the second term is the energy of the guided photon modes, and the third term is the coupling between the emitters and the guided photon modes. Here N is the number of emitters coupled to the 1D waveguide, and r_j is the position of the jth emitter. σ_j^+ and σ_j^- represent the raising and lowering operators of the

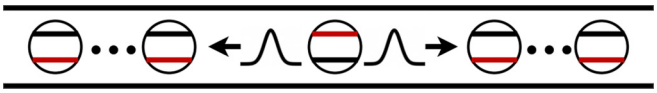

FIG. 1. A two-level emitter is located in an atomic cavity with two N-atom mirrors coupled to a one-dimensional waveguide. The middle emitter is initially in the excited state. The distance between the ith and the jth emitters is r_{ij}. The other emitters are initially in ground states.

jth emitter located at r_j, which provide $\sigma_j^z = [\sigma_j^+, \sigma_j^-]$. γ is the spontaneous decay rate of the emitters to the nonguided modes, a_k and $a_k^\dagger$ are the annihilation and creation operators, and g_k^j is the coupling strength between the guided mode and the jth emitter. To apply the linearized dispersion relation, we assume that the atomic transition frequency ω_a is far from the cutoff frequency of the waveguide and that the photonic spectrum is narrow, i.e., $\delta\omega_k = \omega_k - \omega_a = (|k| - k_a)v_g$ [61].

For the single-photon situation, the atom-field quantum state is given by $|\Psi(t)\rangle = \sum_{j=1}^N \alpha_j(t)e^{-i\omega_a t}|e_j, 0\rangle + \sum_k \beta_k(t)e^{-i\omega_k t}|g, 1_k\rangle$, where $\alpha_j(t)$ is the excitation probability of the jth emitter, and $\beta_k(t)$ is the photon spectrum. From the Schrödinger equation and by integrating the photonic parts, one can obtain the dynamics of the atomic system, which is given by [46]

$$\dot{\alpha}_j(t) = -\frac{1}{2}\sum_{l=1}^{N}(\Gamma e^{ik_a r_{jl}} + \gamma\delta_{jl})\alpha_l\left(t - \frac{r_{jl}}{v_g}\right). \tag{2}$$

The coupling strength between the emitters and the guided photon is determined as $\Gamma = 2L|g_{k_a}|^2/v_g$. In the above equations, the second term includes the collective interaction among the emitters. The time-retarded term shows that the collective interactions induced by the guided photon are long-range effects.

We can then obtain the photon spectra for the right and left propagating fields at $t \to \infty$ [46],

$$\beta_{\delta k}^R(t \to \infty) = -i\sqrt{\frac{\Gamma v_g}{2L}}\sum_{j=1}^{N} e^{-i(k_a+\delta k)r_j}\chi_j(\delta k), \tag{3}$$

$$\beta_{\delta k}^L(t \to \infty) = -i\sqrt{\frac{\Gamma v_g}{2L}}\sum_{j=1}^{N} e^{i(k_a+\delta k)r_j}\chi_j(\delta k), \tag{4}$$

where χ_j is defined as $\chi_j = \int_{-\infty}^{\infty}\alpha_j(t)e^{i\delta k v_g t}dt$, and it is given by

$$\chi_j(\delta k) = \sum_{l=1}^{N} M_{jl}^{-1}(\delta k)A_l(\delta k),$$

with

$$M(\delta k) = \frac{\Gamma}{2}\begin{bmatrix} 1 & e^{ikr_{12}} & \cdots & e^{ikr_{1N}} \\ e^{ikr_{21}} & 1 & \cdots & e^{ikr_{2N}} \\ \vdots & \vdots & \ddots & \vdots \\ e^{ikr_{N1}} & e^{ikr_{N2}} & \cdots & 1 \end{bmatrix} + \left(\frac{\gamma}{2} - i\delta k v_g\right)I_N,$$

$$A_l(\delta k) = \alpha_l(0), \tag{5}$$

where $r_{ij} = |r_i - r_j|$ represents the distance between the ith and the jth emitters.

The remaining probability amplitude inside the cavity can be estimated based on $R_{\delta k}$, the effective reflectivity of the atomic mirrors. After N reflections, the probability amplitude inside the cavity is approximately [59]

$$P(t) = \int_{-\infty}^{\infty} d\delta k|\beta_{\delta k}(0)|^2 R_{\delta k}^N,$$

with

$$\beta_{\delta k}(0) = -i\sqrt{\frac{\Gamma v_g}{2L}}\frac{2}{\Gamma + \gamma - 2i\delta k v_g}, \tag{6}$$

where $N(t)$ denotes the Nth interaction at time t. $\beta_{\delta k}(0)$ is the initial emission spectrum in the absence of atomic mirrors. The effective reflectivity of the atomic mirrors varies with the number of atoms and the distance between them [58].

In this section, we consider the excitation of emitters inside the cavity of single-atom mirrors. We assume that the emitter in the middle is initially in the excited state, while the emitters on the left and right are initially in the ground state, i.e., $\alpha_1(0) = \alpha_3(0) = b_j = 0, \alpha_2(0) = 1$.

In Fig. 2(a), we show the excitation probabilities of the emitters. The dashed red line with asterisk markers shows the excitation probability of the middle emitter, which is similar to the phenomena of an excited emitter in a damped cavity [62]. The dashed blue line with triangle markers corresponds to the excitation probability of the side emitters. Since the system is symmetric, the side emitters share the same dynamics. The probability amplitude remaining inside the cavity is shown by the solid black line, while the estimate based on Eq. (6) is depicted by the dash-dotted black line with effective reflectivity $R_{\delta k} = \Gamma^2/[(\Gamma + \gamma)^2 + 4\delta k^2 v_g^2]$, which agrees well with the simulation result. The dotted black line with diamond markers shows the spontaneous decay of a single emitter without atomic mirrors, i.e., $e^{-\Gamma t}$. Comparing the excitation probability of the middle emitter and the spontaneous decay of a single emitter, it is evident that the atomic arrays act like mirrors in the conventional cavities, which significantly slow down the decay of the photon in the cavity. Here we take $l = 0.5\lambda$. Note that a larger distance would lead to similar results, since the phase matters more than the distance. With $v_g t/L$ as the x-axis instead of γt, the freedom to place atoms at greater distances becomes possible, ruling out the effect of the propagating time of the photon between the mirrors.

We present the photon emission spectra of the case with an excited emitter and two single-atom mirrors in Fig. 2(b). Here, we ignore the decay into nonguided modes $\gamma = 0$ and set the separations between the emitters as $r_{i,i+1} = l = \lambda$, where λ is the wavelength corresponding to the transition frequency of the two-level emitters. The red solid line is the left and right propagating spectra, which overlap due to the symmetry. For comparison, the black dashed line shows the emission spectra of a single excited emitter without the atomic cavity. Only a discrete subset of photon frequencies can be transmitted through the cavity, and the transmitted frequencies are nearly equally spaced. Similar to a frequency comb, these frequencies can be useful for precision measurements. A similar frequency comb can be generated by a single photon initially excited inside or outside an atomic cavity [58]. In Fig. 2(c), we choose asymmetric separations for the left and right emitters,

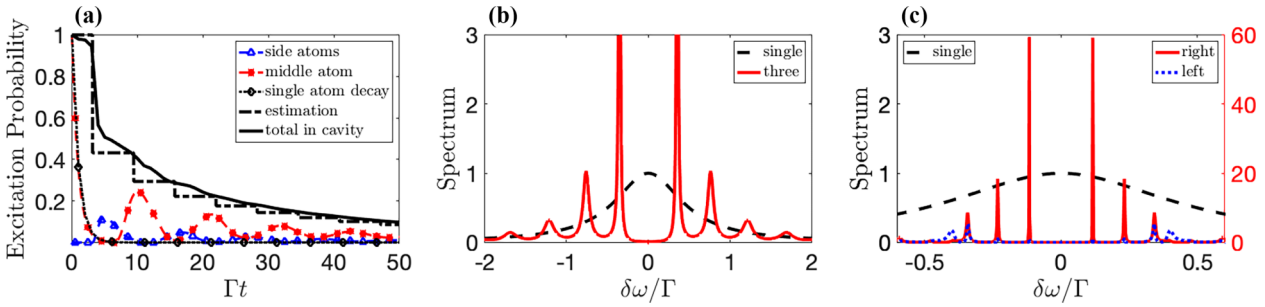

FIG. 2. (a) The excitation probabilities of three emitters with the middle one initially in the excited state, with $\gamma = 0.05, l = 0.5\lambda$. (b) The spectrum of the photon with the middle emitter initially in the excited state, with $\gamma = 0, l = 1\lambda$. (c) The spectrum of the left-propagating and right-propagating parts of the photon with the middle emitter initially in the excited state, with $\gamma = 0, r_{12} = 1\lambda, r_{23} = 4\lambda$. The black dashed line, scaled by the left Y-axis, is the spectrum of the single-photon case without the atomic cavity. The red solid and blue dotted lines, scaled by the right Y-axis, are the spectra of the right- and left-propagating parts of the photon.

e.g., $r_{12} = \lambda, r_{23} = 4\lambda$. Scaled by the right Y-axis, the red solid line shows the right propagating spectrum, and the blue dotted line represents the left propagating spectrum. Due to the asymmetry, the spectra of the right and left propagating parts no longer overlap, while the amplitudes of the comb lines are significantly enhanced compared to the symmetric case. By choosing asymmetric parameters, the frequency comb in the left direction is suppressed and eliminated. However, the frequency comb in the right direction is significantly enhanced and becomes more uniformly distributed by simply changing the atomic spacing on one side.

III. SPECTRUM NARROWING

The photon emission spectra can vary greatly by different choices of the separations between the emitters. Here we show that we can narrow the emission spectra by choosing smaller separations.

As shown in Fig. 3(a), the narrowed spectrum is represented by the red solid line, where $r_{i,i+1} = l = 0.01\lambda$. The black dashed line shows the single-emitter emission spectra without the atomic cavity. With the same separations on both sides, the right and left propagating parts overlap. The emission spectrum narrows near the resonance, while the amplitude enhances. The asymmetric spectrum in Fig. 3(a) peaks near the resonant frequency with a Fano-like line shape, which has also been observed in some other waveguide systems [28,50,63].

We also consider the asymmetric scenarios by setting different atomic transition frequencies. Considering the off-resonant case, the larger the off-resonance, the smaller the excitation probability of the emitter, which means that the quality of the cavity reduces in this case. In Fig. 3(b), we show the narrowed spectra generated with the red solid and blue dotted lines corresponding to the right and left propagating parts, respectively. In this setting, we choose $l = 0.1\lambda, k_1 = k_2, k_3 = 1.05k_2$, where k_i is the wave vector corresponding to the transition frequency of the ith emitter. In this case, we obtain unidirectional spectral narrowing.

Here we derive the analytical expressions of the emission spectra for the single-atom mirror setting, where the matrix $M(\delta k)$ is

$$M(\delta k) = \frac{\Gamma}{2}\begin{bmatrix} 1 & e^{ikr_{12}} & e^{ikr_{13}} \\ e^{ikr_{21}} & 1 & e^{ikr_{23}} \\ e^{ikr_{31}} & e^{ikr_{32}} & 1 \end{bmatrix} + \left(\frac{\gamma}{2} - i\delta k v_g\right) I_3. \tag{7}$$

Assuming that the atomic separations are equal, $r_{i,i+1} = l$, the inverse of the matrix is

$$M^{-1}(\delta k) = \frac{2}{\Gamma}\begin{bmatrix} G_1 & G_4 & G_2 \\ G_4 & G_3 & G_4 \\ G_2 & G_4 & G_1 \end{bmatrix}, \tag{8}$$

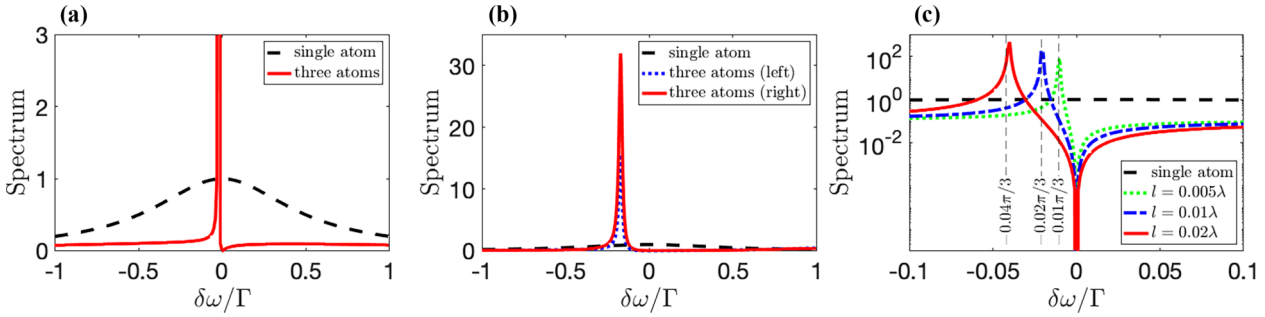

FIG. 3. (a) The spectrum of the photon with the middle emitter initially in the excited state, with $\gamma = 0, l = 0.01\lambda$. (b) The spectrum of the left- and right-propagating parts of the photon with the middle emitter initially in the excited state, with $\gamma = 0, l = 0.1\lambda, k_1 = k_2, k_3 = 1.05k_2$. (c) The closeup of the narrowed spectra shows the modulation of the central frequencies by changing the atomic spacing.

where

$$G_1 = \frac{1}{A}\left[\left(\frac{\gamma}{\Gamma}+1\right)^2 - e^{2ikl} - \frac{4\delta k v_g}{\Gamma}\left(i\frac{\gamma}{\Gamma}+i+\frac{\delta k v_g}{\Gamma}\right)\right],$$
$$G_2 = \frac{1}{A}\left(i\frac{2\delta k v_g}{\Gamma}-\frac{\gamma}{\Gamma}\right)e^{2ikl},$$
$$G_3 = \frac{1}{B}\left(-1-e^{2ikl}+i\frac{2\delta k v_g}{\Gamma}-\frac{\gamma}{\Gamma}\right),$$
$$G_4 = \frac{1}{B}e^{ikl}, \tag{9}$$

with

$$A = \left(\frac{\gamma}{\Gamma}+1-i\frac{2\delta k v_g}{\Gamma}\right)^3 - \left(\frac{\gamma}{\Gamma}+1-i\frac{2\delta k v_g}{\Gamma}\right)(e^{2ikl}+1)^2 + \frac{\gamma}{\Gamma}+1-i\frac{2\delta k v_g}{\Gamma}+2e^{4ikl},$$
$$B = \left(\frac{2\delta k v_g}{\Gamma}+i\frac{\gamma}{\Gamma}\right)^2 + i\left(\frac{2\delta k v_g}{\Gamma}+i\frac{\gamma}{\Gamma}\right)(e^{2ikl}+2)+e^{2ikl}-1. \tag{10}$$

Based on the initial condition, we have $\alpha_1(0)=\alpha_3(0)=0, \alpha_2(0)=1$. Substituting $M^{-1}(\delta k)$ into Eqs. (3) and (4), we derive the emission spectra

$$\beta^R_{\delta k}(t\to\infty) = -i\sqrt{\frac{2v_g}{\Gamma L}}(e^{-ikr_1}G_4 + e^{-ikr_2}G_3 + e^{-ikr_3}G_4),$$
$$\beta^L_{\delta k}(t\to\infty) = -i\sqrt{\frac{2v_g}{\Gamma L}}(e^{ikr_1}G_4 + e^{ikr_2}G_3 + e^{ikr_3}G_4). \tag{11}$$

The positions of the peaks coincide with the singularity points given by the roots of the denominator. Considering the approximation $kl \ll 1$ with $\gamma = 0$, we derive the position of the peak in the spectra

$$\frac{\delta k v_g}{\Gamma} = \frac{\delta\omega}{\Gamma} = -\frac{kl}{3}, \tag{12}$$

which shows that the deviation of the central frequency from the resonance is proportional to the atomic spacing l. Under this approximation condition, we can control the central frequency of the narrowed output spectra by modulating the atomic spacing as illustrated in Fig. 3(c). The black line shows the single emitter emission spectrum with the atomic cavity absent. The green dotted, blue dash-dotted, and red solid lines are the emission spectra with $l = 0.005\lambda, 0.01\lambda, 0.02\lambda$, respectively. The vertical dashed lines are the prediction of central frequencies given by Eq. (12). Practical constraints may hinder the attainment of perfect atomic spacings, potentially leading to minor fluctuations in the central frequency of the narrowed spectrum. Nonetheless, our analysis suggests a tolerance range within which the modulation of atomic spacing retains its effect on the central frequency. Minor deviations due to imperfect atomic spacings are expected, but our principal findings remain largely robust within the tolerance range.

IV. ENTANGLEMENT

Due to the collective interaction among the emitters, quantum entanglement can be generated through the propagation of photons [37,64–67]. The quantum entanglement of a two-qubit system can be quantified by the concurrence, which is defined as

$$C(\rho) = \max\{0, \lambda_1-\lambda_2-\lambda_3-\lambda_4\}, \tag{13}$$

where λ_i are the eigenvalues, in decreasing order, of the Hermitian matrix $\Lambda = \sqrt{\sqrt{\rho}\tilde{\rho}\sqrt{\rho}}$ with the spin-flipped state $\tilde{\rho} = (\sigma_y\otimes\sigma_y)\rho^*(\sigma_y\otimes\sigma_y)$. The density matrix of the system is $\rho_{AF}(t) = |\Psi(t)\rangle\langle\Psi(t)|$. After tracing over the photonic parts, the density matrix of the atomic system is $\rho_A(t) = \mathrm{Tr}_F[\rho_{AF}(t)]$. By tracing over the middle emitter, the density matrix can be reduced to the bipartite entanglement between the left and the right emitters,

$$\rho_{\mathrm{bi}}(t) = \mathrm{Tr}_{\mathrm{atom}_2}[\rho_A(t)] = \begin{bmatrix} \sum_k|\beta_k(t)|^2 & 0 & 0 & 0 \\ 0 & |\alpha_1(t)|^2 & \alpha_1(t)\alpha_3^*(t) & 0 \\ 0 & \alpha_1^*(t)\alpha_3(t) & |\alpha_3(t)|^2 & 0 \\ 0 & 0 & 0 & 0 \end{bmatrix}. \tag{14}$$

Thus, the Hermitian matrix $\Lambda(t)$ is given by

$$\Lambda(t) = \frac{2|\alpha_1(t)||\alpha_3(t)|}{|\alpha_1(t)|^2+|\alpha_3(t)|^2} \times \begin{bmatrix} 0 & 0 & 0 & 0 \\ 0 & |\alpha_1(t)|^2 & \alpha_1(t)\alpha_3(t)^* & 0 \\ 0 & \alpha_1^*(t)\alpha_3(t) & |\alpha_3(t)|^2 & 0 \\ 0 & 0 & 0 & 0 \end{bmatrix}, \tag{15}$$

and its eigenvalues are $\lambda_1 = 2|\alpha_1(t)\alpha_3(t)^*|$, $\lambda_2=\lambda_3=\lambda_4=0$. Hence the time-dependent concurrence of bipartite entanglement is derived as

$$C(t) = \max\{0, 2|\alpha_1(t)\alpha_3(t)^*|\}, \tag{16}$$

where $C(t)$ denotes the bipartite concurrence of the two-atom system at time t. As can be seen from this equation, the concurrence is proportional to the roots of the excitation probabilities of the two side emitters. Quantum entanglement between the two emitters can be generated as the photons propagate through. In Fig. 4, we present the concurrence of the bipartite entanglement between the left and the right emitter with separation $l = \lambda$. The solid black line shows the case ignoring the spontaneous decay into nonguided modes.

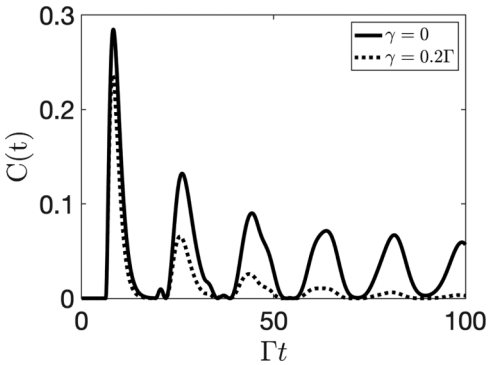

FIG. 4. The concurrence of the bipartite entanglement between the left and the right emitters (the mirrors), for $l = \lambda$.

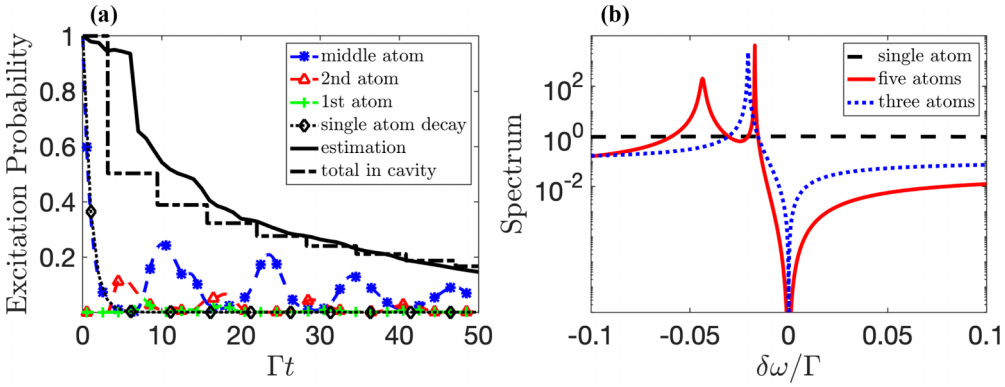

FIG. 5. (a) The excitation probabilities of five emitters, with the middle one initially in the excited state, with $\gamma = 0.05\Gamma$, $l = 0.5\lambda$. (b) The narrowed spectrum with the middle emitter initially in the excited state, with $\gamma = 0, l = 0.01\lambda$. The black dashed line is the spectrum of the single-photon case without the atomic cavity. The red solid and blue dotted lines are the spectra of the outgoing photon in the cases with single- and two-atom mirrors.

The dashed black line shows the case with $\gamma = 0.2\Gamma$, which decays much faster compared to the case with $\gamma = 0$. Since the entanglement is generated as the photon propagates, we observe the entanglement sudden birth and revival of entanglement by choosing larger atomic separations. The sudden birth of the entanglement occurs when the photon reaches the side emitters. The entanglement diminishes along with the spontaneous decay of two side emitters. When the reflected part of the photon travels back to the side emitters, we observe the revival of the entanglement. A smaller spontaneous decay rate γ preserves the bipartite entanglement for a longer time.

V. MULTIPLE-ATOM MIRRORS

Recently, it has been shown that one can obtain an atomic cavity with higher finesse by adding more emitters to the mirrors. In this section, we discuss the single-photon emission inside an atomic cavity with multiatom mirrors.

In Fig. 5(a), we show the decay of the excitation with two-atom mirrors. The atomic separation is taken to be $l = 0.5\lambda$, and the spontaneous decay rate to the nonguided modes is chosen to be $\gamma = 0.05\Gamma$. The dashed blue line with asterisk markers is the excitation probability of the middle emitter. The red dashed line with triangle markers and the green line with plus sign markers are for the second and third emitters away from the middle. Due to the symmetry, the dynamics on the right and the left sides overlap. The dotted black line with diamond markers shows the spontaneous decay of a single emitter without atomic mirrors, i.e., $e^{-\Gamma t}$. The probability amplitude remaining inside the cavity is shown by the solid black line, while the estimate based on Eq. (6) is depicted by the dash-dotted black line with effective reflectivity [58]

$$R_{\delta k} = \left| \frac{\eta_\Gamma (1 + e^{2ika})(1 - i\eta_{\delta k}) - 2\eta_\Gamma^2 e^{2ika}}{(1 - i\eta_{\delta k})^2 - \eta_\Gamma^2 e^{2ika}} \right|^2, \tag{17}$$

where $\eta_\Gamma = 1/(1 + \gamma/\Gamma)$, $\eta_{\delta k} = 2\delta k v_g/(\Gamma + \gamma)$. a is the distance between the mirror atoms. The spectrum is shown in Fig. 5(b), where the black dashed line represents the emission spectrum of a single excited emitter without the atomic cavity. The red solid line is for the two-atom-mirror case, and the black dotted line is for the single-atom case. The decay of the photon is much slower than in the case of a single-atom cavity. Adding more emitters to the mirrors does not dramatically increase the finesse of the cavity in this setting. Therefore, the two-atom mirrors are optimal for a high-finesse cavity in terms of single-photon emission. The spectra are narrowed by the presence of the atomic cavity. Note that an additional emitter in the mirror induces the bifurcation of the narrowed spectra, as shown in Fig. 5(b). The blue dotted line is for the two-atom-mirror case. In the single-atom-mirror case, the peaks of the narrowed spectra appear at the singularity points in the expressions of the spectra. By adding an extra emitter to the mirrors, we introduce an extra singularity point into the expressions of the spectra.

VI. CONCLUSION

In this paper, we studied the single-photon emission inside an atomic cavity coupled to a one-dimensional waveguide. Due to the collectively enhanced coupling, the atomic cavity preserves the single photon, similar to a damped cavity. With a proper choice of atomic spacing, we can realize a single-photon frequency comb, spectrum narrowing, and unidirectional spectrum narrowing. Within a certain range, we can control the central frequency of the narrowed spectrum by modulating the atomic spacing. The sudden birth and revival of the bipartite entanglement followed by asymptotic decay are observed alongside the photon propagating back and forth.

ACKNOWLEDGMENTS

This research is supported by the project NPRP 13S-0205-200258 of the Qatar National Research Fund (QNRF). C.Z. is supported by the HEEP fellowship. Z.L. is supported by the Key-Area Research and Development Program of Guangdong Province (Grant No. 2018B030329001), the National Key R&D Program of China (Grant No. 2021YFA1400800), and the Natural Science Foundations of Guangdong (Grant No. 2021A1515010039).

[1] T. Northup and R. Blatt, Nat. Photon. **8**, 356 (2014).
[2] P. Domokos, J.-M. Raimond, M. Brune, and S. Haroche, Phys. Rev. A **52**, 3554 (1995).
[3] A. Barenco, D. Deutsch, A. Ekert, and R. Jozsa, Phys. Rev. Lett. **74**, 4083 (1995).
[4] T. Pellizzari, S. A. Gardiner, J. I. Cirac, and P. Zoller, Phys. Rev. Lett. **75**, 3788 (1995).
[5] H. J. Kimble, Phys. Scr. **T76**, 127 (1998).
[6] J. Ye, D. W. Vernooy, and H. J. Kimble, Phys. Rev. Lett. **83**, 4987 (1999).
[7] S.-B. Zheng and G.-C. Guo, Phys. Rev. Lett. **85**, 2392 (2000).
[8] A. Blais, R.-S. Huang, A. Wallraff, S. M. Girvin, and R. J. Schoelkopf, Phys. Rev. A **69**, 062320 (2004).
[9] H. Dong, Z. R. Gong, H. Ian, and L. Zhou, C. P. Sun, Phys. Rev. A **79**, 063847 (2009).
[10] V. Giovannetti, D. Vitali, P. Tombesi, and A. Ekert, Phys. Rev. A **62**, 032306 (2000).
[11] J. Wang, F. Sciarrino, A. Laing, and M. G. Thompson, Nat. Photon. **14**, 273 (2020).
[12] U. L. Andersen, Nature (London) **591**, 40 (2021).
[13] X. Qiang, X. Zhou, J. Wang, C. M. Wilkes, T. Loke, S. O'Gara, L. Kling, G. D. Marshall, R. Santagati, T. C. Ralph *et al.*, Nat. Photon. **12**, 534 (2018).
[14] E. M. Purcell, H. C. Torrey, and H. C. Torrey R. V. Pound, Phys. Rev. **69**, 37 (1946).
[15] L. Scarpelli, B. Lang, F. Masia, D. M. Beggs, E. A. Muljarov, A. B. Young, R. Oulton, M. Kamp, S. Höfling, C. Schneider, and W. Langbein, Phys. Rev. B **100**, 035311 (2019).
[16] H. J. Kimble, Nature (London) **453**, 1023 (2008).
[17] H. Pichler, T. Ramos, A. J. Daley, and P. Zoller, Phys. Rev. A **91**, 042116 (2015).
[18] S. Mahmoodian, P. Lodahl, and A. S. Sørensen, Phys. Rev. Lett. **117**, 240501 (2016).
[19] T. Ramos, B. Vermersch, P. Hauke, H. Pichler, and P. Zoller, Phys. Rev. A **93**, 062104 (2016).
[20] H. Zheng, D. J. Gauthier, and H. U. Baranger, Phys. Rev. Lett. **111**, 090502 (2013).
[21] V. Paulisch, H. Kimble, and A. González-Tudela, New J. Phys. **18**, 043041 (2016).
[22] Z. Liao and M. S. Zubairy, Phys. Rev. A **98**, 023815 (2018).
[23] J.-Q. Liao, J.-F. Huang, Y.-x. Liu, L.-M. Kuang, and C. P. Sun, Phys. Rev. A **80**, 014301 (2009).
[24] D.-C. Yang, M.-T. Cheng, X.-S. Ma, J. Xu, C. Zhu, and X.-S. Huang, Phys. Rev. A **98**, 063809 (2018).
[25] T. Li, A. Miranowicz, X. Hu, K. Xia, and F. Nori, Phys. Rev. A **97**, 062318 (2018).
[26] Y. Lu, Z. Liao, F.-L. Li, and X.-H. Wang, Photon. Res. **10**, 389 (2022).
[27] J.-T. Shen and S. Fan, Opt. Lett. **30**, 2001 (2005).
[28] J.-T. Shen and S. Fan, Phys. Rev. Lett. **95**, 213001 (2005).
[29] J.-F. Huang, T. Shi, C. P. Sun, F. Nori *et al.*, Phys. Rev. A **88**, 013836 (2013).
[30] S. Fan, Ş. E. Kocabaş, and J.-T. Shen, Phys. Rev. A **82**, 063821 (2010).
[31] K. Lalumiere, B. C. Sanders, A. F. van Loo, A. Fedorov, A. Wallraff, and A. Blais, Phys. Rev. A **88**, 043806 (2013).
[32] E. Rephaeli, J.-T. Shen, and S. Fan, Phys. Rev. A **82**, 033804 (2010).
[33] Y. Chen, M. Wubs, J. Mørk, and A. F. Koenderink, New J. Phys. **13**, 103010 (2011).
[34] Q. Li, L. Zhou, and C. P. Sun, Phys. Rev. A **89**, 063810 (2014).
[35] T. S. Tsoi and C. K. Law, Phys. Rev. A **78**, 063832 (2008).
[36] P. Lodahl, S. Mahmoodian, and S. Stobbe, Rev. Mod. Phys. **87**, 347 (2015).
[37] Z. Liao, X. Zeng, H. Nha, and M. S. Zubairy, Phys. Scr. **91**, 063004 (2016).
[38] D. Roy, C. M. Wilson, and O. Firstenberg, Rev. Mod. Phys. **89**, 021001 (2017).
[39] D. E. Chang, J. S. Douglas, A. González-Tudela, C.-L. Hung, and H. J. Kimble, Rev. Mod. Phys. **90**, 031002 (2018).
[40] S. Samimi and M. M. Golshan, Phys. Rev. A **105**, 053702 (2022).
[41] J.-Q. Liao and C. K. Law, Phys. Rev. A **82**, 053836 (2010).
[42] Z. Liao, Y. Lu, and M. S. Zubairy, Phys. Rev. A **102**, 053702 (2020).
[43] K. L. Tsakmakidis, P. K. Jha, Y. Wang, and X. Zhang, Sci. Adv. **4**, eaaq0465 (2018).
[44] S. Mahmoodian, M. Čepulkovskis, S. Das, P. Lodahl, K. Hammerer, and A. S. Sørensen, Phys. Rev. Lett. **121**, 143601 (2018).
[45] A. González-Tudela, V. Paulisch, D. E. Chang, H. J. Kimble, and J. I. Cirac, Phys. Rev. Lett. **115**, 163603 (2015).
[46] Z. Liao, X. Zeng, S.-Y. Zhu, and M. S. Zubairy, Phys. Rev. A **92**, 023806 (2015).
[47] J. S. Douglas, H. Habibian, C.-L. Hung, A. V. Gorshkov, H. J. Kimble, and D. E. Chang, Nat. Photon. **9**, 326 (2015).
[48] J. D. Hood, A. Goban, A. Asenjo-Garcia, M. Lu, S.-P. Yu, D. E. Chang, and H. Kimble, Proc. Natl. Acad. Sci. USA **113**, 10507 (2016).
[49] M.-T. Cheng, J. Xu, and G. S. Agarwal, Phys. Rev. A **95**, 053807 (2017).
[50] Z. Liao, H. Nha, and M. S. Zubairy, Phys. Rev. A **94**, 053842 (2016).
[51] Z. Liao and M. S. Zubairy, Phys. Rev. A **90**, 053805 (2014).
[52] A. A. Svidzinsky, J.-T. Chang, and M. O. Scully, Phys. Rev. A **81**, 053821 (2010).
[53] M. O. Scully and A. A. Svidzinsky, Science **325**, 1510 (2009).
[54] A. Albrecht, L. Henriet, A. Asenjo-Garcia, P. B. Dieterle, O. Painter, and D. E. Chang, New J. Phys. **21**, 025003 (2019).
[55] D. E. Chang, L. Jiang, A. Gorshkov, and H. Kimble, New J. Phys. **14**, 063003 (2012).
[56] M. Mirhosseini, E. Kim, X. Zhang, A. Sipahigil, P. B. Dieterle, A. J. Keller, A. Asenjo-Garcia, D. E. Chang, and O. Painter, Nature (London) **569**, 692 (2019).
[57] P.-O. Guimond, A. Roulet, H. N. Le, and V. Scarani, Phys. Rev. A **93**, 023808 (2016).
[58] Z. Liao, H. Nha, and M. S. Zubairy, Phys. Rev. A **93**, 033851 (2016).
[59] C. Zhou, Z. Liao, and M. S. Zubairy, Phys. Rev. A **105**, 033705 (2022).
[60] Y. Lu, S. Gao, A. Fang, Z. Liao, and F. Li, Phys. Lett. A **382**, 1823 (2018).
[61] J.-T. Shen and S. Fan, Phys. Rev. A **79**, 023837 (2009).
[62] M. O. Scully and M. S. Zubairy, *Quantum Optics* (Cambridge University Press, Cambridge, 1997).

[63] M.-T. Cheng and Y.-Y. Song, Opt. Lett. **37**, 978 (2012).
[64] S. A. Hill and W. K. Wootters, Phys. Rev. Lett. **78**, 5022 (1997).
[65] W. K. Wootters, Phys. Rev. Lett. **80**, 2245 (1998).
[66] H. Zheng and H. U. Baranger, Phys. Rev. Lett. **110**, 113601 (2013).
[67] A. González-Tudela and D. Porras, Phys. Rev. Lett. **110**, 080502 (2013).